Springer

KSME

Journal of Mechanical Science and Technology 24 (3) (2010) 761~767
www.springerlink.com/content/1738-494x
DOI 10.1007/s12206-010-0202-1

An investigation on the integrated human driver model for closed-loop simulation of intelligent safety systems †

Taeyoung Lee[1], Juyong Kang[1], Kyongsu Yi[1,*] and Kihan Noh[2]

[1]*School of Mechanical and Aerospace Engineering, Seoul National University, Seoul, 151-742, Korea*
[2]*Vehicle Platform Research Center, Korea Automotive Technology Institute (KATECH), Chonan, 330-912, Korea*

(Manuscript Received March 2, 2009; Revised September 28, 2009; Accepted January 29, 2010)

Abstract

This paper presents an integrated human driver model for a closed-loop simulation of the intelligent safety system. A lateral human driver model was developed to represent the steering behavior of a human driver using the finite preview optimal control method. A longitudinal human driver model represents a human driver's throttle and brake control behavior relative to the preceding vehicle motion. It computes the desired acceleration and generates throttle/brake inputs to maintain vehicle-to-vehicle clearance at a desired level or to control vehicle speed. An integrated driver model was been developed using the longitudinal and lateral driver models to represent the behavior of a human driver in alternative driving situations, that is, vehicle following, lane following, emergency braking, and so on. Simulation studies were conducted using "Carsim" model which is validated using vehicle test data. Results showed that a human driver's behaviors could be well represented by the integrated human driver model presented in this paper. Closed-loop simulations of a unified chassis control system with the integrated human driver model were conducted.

Keywords: Human driver model; Finite optimal preview control; Closed-loop simulation; Unified chassis control

1. Introduction

The demand for vehicle control systems is currently shifting from the realization of high performance vehicles to the development of safety systems such as Electronic Stability Control (ESC), Adaptive Cruise Control (ACC), Unified Chassis Control (UCC), and so on, and human-friendly vehicle control systems. The evaluation of vehicle active safety systems also relies on field testing which is time-consuming, expensive, and sometimes dangerous. Therefore, closed human-in-the-loop evaluation would be a more effective way to assess vehicle active safety systems than the general open-loop evaluation based on prescribed steering and velocity profiles.

Many ideas have been exploited for the driver model. The common idea in these works is the nonlinear and/or stochastic modeling of human behavior such as neural networks (NN) [1] and, hidden Markov models (HMM) [2]. These techniques, however, have some underlying problems. First, the obtained model is often very complicated. Second, they make it impossible to understand the physical meaning of the driving behavior. Another idea is that the driver is regarded as a kind of "controller". The linear control theory has been applied to analyze the driving behavior, steering control behavior and throttle/brake control behavior [3].

Hedrick [4] and Rajamani [5] conducted research works on the combined model of the driver's longitudinal and lateral control behavior. However, these papers treat the model as applied in restricted driving conditions, while evaluation through another research has not yet been developed.

This paper presents the development of an integrated human driver model for closed-loop simulation of an intelligent safety system. To represent the steering behavior of a human driver, the lateral human driver model uses a finite preview optimal control method. A longitudinal human driver model represents a human driver's throttle and brake control behavior based on the analysis of manual driving data. A curvature-based human driver model has been used to represent a throttle/brake motion relative to road curvature information. The integrated human driver model controls the vehicle to provide realistic vehicle behavior similar to the normal driving of a real human driver.

2. Development of the integrated human driver model

The integrated human driver model consists of three parts, lateral human driver model, longitudinal human driver model,

† This paper was recommended for publication in revised form by Associate Editor Jong Hyeon Park

*Corresponding author. Tel.: +82 2 880 1941, Fax.: +82 2 880 1942
E-mail address: kyi@snu.ac.kr

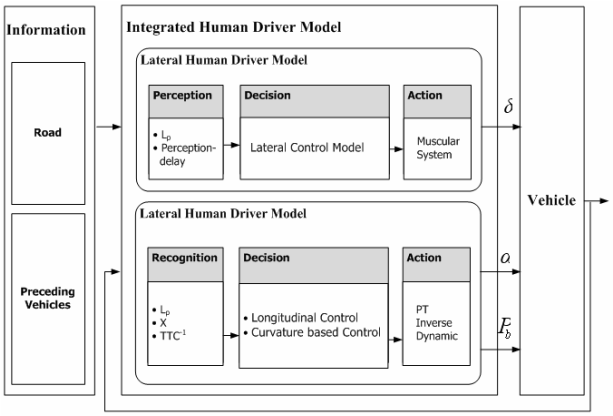

Fig. 1. Structure of an integrated human driver model.

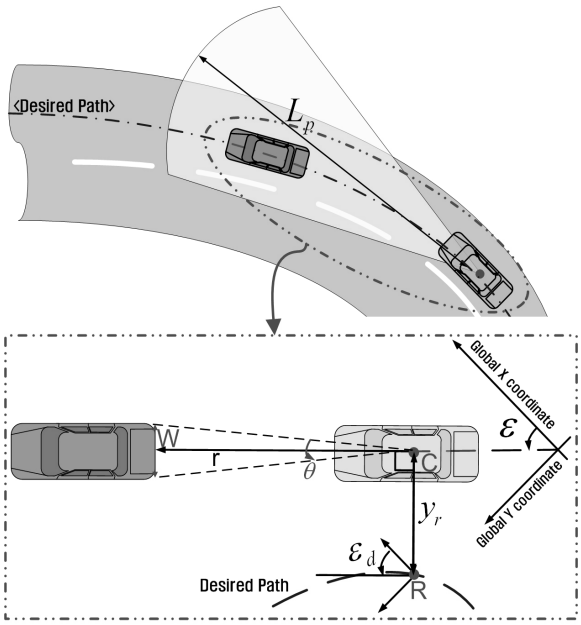

Fig. 2. Driver-vehicle-road relation system.

and curvature-based human driver model. The overall structure is shown in Fig. 1.

Fig. 2 shows the driver-vehicle-road relation system. Lateral position error (y_r) is the lateral distance between the vehicle C.G (C) and the centerline of the desired path (R) (Fig. 2). Yaw angle error ($\varepsilon - \varepsilon_d$) is determined using the yaw angle of the vehicle (ε) and the desired yaw angle as dictated by the desired path (ε_d) [6].

To represent the relations between a preceding vehicle and a subject vehicle, the preceding vehicle's width (w), driver's view angle (θ), and clearance between the preceding vehicle end point and driver's eye (r_d) were determined. The rate of change of the lateral position error (y_r) and yaw angle error ($\varepsilon - \varepsilon_d$) were determined, as in (1) and (2), [7]

$$\dot{y}_r = v_y + v_x \cdot (\varepsilon - \varepsilon_d) \tag{1}$$

$$\dot{\varepsilon}_d = \frac{v_x}{R} \tag{2}$$

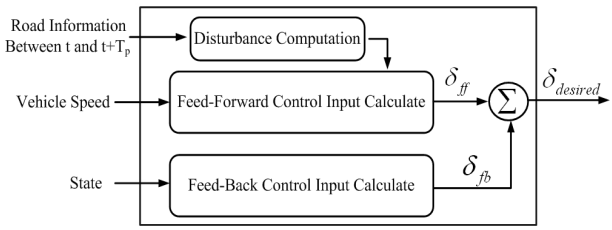

Fig. 3. Structure of the lateral human driver model.

where R denotes the radius of the desired path.

L_p is the driver's preview distance. A preview distance map with respect to road curvature and vehicle velocity was used to represent the driver's preview distance. The distance map was constructed based on a real driver's manual driving data.

The width of the preceding vehicle, w, is constant and can be represented as the driver's view angle (θ) and clearance (r):

$$w = r \cdot \theta \tag{3}$$

2.1 Lateral human driver model

The Lateral Human Driver Model's overall structure is shown in Fig. 3. A Finite Preview Optimal Control method was used to design the Later Human Driver Model. To develop the lateral human driver model using the finite preview control theory, the preview distance was transformed into preview time (T_p) as in (4).

$$T_p = \frac{L_p}{v_x} \tag{4}$$

In using the finite preview optimal control method, the control input [$\delta_f(t)$] consists of the Feed-back Control Input and Feed-forward Control Input. It can deal with both the current vehicle state and road information beyond the preview distance (L_p).

In the lateral human driver model, the lateral position error (y_r), yaw angle error ($\varepsilon - \varepsilon_d$) and rate of change of these two values constitute a state (X). A state Eq. (5) can be obtained by substituting a 2-DOF bicycle model's dynamic equation and a linear tire model's lateral tire force equations [8].

$$\begin{aligned} \dot{X} &= A \cdot X + B \cdot \delta_f + F_d \cdot w_d \\ X &= [y_r \quad \dot{y}_r \quad \varepsilon - \varepsilon_d \quad \dot{\varepsilon} - \dot{\varepsilon}_d]^T \end{aligned} \tag{5}$$

where

$$A = \begin{bmatrix} 0 & 1 & 0 & 0 \\ 0 & \frac{A_1}{v_x} & -A_1 & \frac{A_2}{v_x} \\ 0 & 0 & 0 & 1 \\ 0 & \frac{A_3}{v_x} & -A_3 & \frac{A_4}{v_x} \end{bmatrix} \quad B = \begin{bmatrix} 0 \\ B_1 \\ 0 \\ B_2 \end{bmatrix}$$

$$F_d = \begin{bmatrix} 0 & 0 \\ 1 & 0 \\ 0 & 0 \\ 0 & 1 \end{bmatrix} \qquad w_d = \begin{bmatrix} d_1 \\ d_2 \end{bmatrix}$$

$$A_1 = \frac{-2\cdot(C_f + C_r)}{m} \qquad A_2 = \frac{2\cdot(-l_f\cdot C_f + l_r\cdot C_r)}{m}$$

$$A_3 = \frac{2\cdot(-l_f\cdot C_f + l_r\cdot C_r)}{I_z} \qquad A_4 = \frac{-2\cdot(l_f^2\cdot C_f + l_r^2\cdot C_r)}{I_z}$$

$$B_1 = \frac{2\cdot C_f}{m} \qquad B_2 = \frac{2\cdot C_f\cdot l_f}{I_z}$$

$$d_1 = -\frac{v_x^2}{\rho} + \frac{A_2}{v_x}\cdot\dot{\varepsilon}_d \qquad d_2 = \frac{A_4}{v_x}\cdot\dot{\varepsilon}_d - \ddot{\varepsilon}_d$$

where m denotes the mass of the body, I_z the yaw moment of inertia, and l_f and l_r the distance from the center of gravity (*C.G*) to the front and rear axles, respectively. C_f and C_r denote the equivalent front and rear cornering stiffness.

The Lateral Human Driver Model's control input [$\delta_f(t)$] was computed to minimize the performance index given in (6) [6].

$$\lim_{t_f\to\infty}\frac{1}{t_f}E\{\int_0^{t_f}\begin{bmatrix}\frac{1}{2}(X^TQX+\delta_f^TR\delta_f)+\\ \lambda^T\cdot(A\cdot X+B\cdot\delta_f+F_d\cdot w_d-\dot{x})\end{bmatrix}dt\} \tag{6}$$

where weighting factors Q and R are relative to the driver's characteristics, gender, driving career, and so on.

The solution that minimizes the performance index was derived through the well-known Euler Lagrange equation [9] and standard LQ Riccati equation [10]. Consequently, the lateral human driver Model's control input was computed as in (7) [11].

$$\begin{aligned}\delta_{desired}(t) &= -K_{opt}\cdot X(t) + M(t)\\ &= \delta_{fb}(t) + \delta_{ff}(t)\end{aligned} \tag{7}$$

where $K_{opt} = \delta_{fb}(t) = -R^{-1}\cdot B^T\cdot P_{ss}$

$$M(t) = \delta_{ff}(t) = -R^{-1}\cdot B^T\cdot\int_0^{T_p}F_1(\xi)\cdot w(t+\xi)\cdot d\xi$$

$$F_1(t) = e^{A_c^T\cdot t}\cdot P_{ss}\cdot F_d$$

2.2 Longitudinal human driver model

The driver's throttle/brake controls relative to a preceding vehicle was decided using the longitudinal human driver model, which consists of two parts, the upper level and lower levels. Fig. 4 presents its structure. The longitudinal human driver model monitors two indexes, x and TTC^{-1}, and determines a driving situation, for example, "safe", "warning" or "dangerous".

The upper-level controller, according to the driving situation, determines the desired acceleration (a_{des_long}). In the safe driving condition, the desired accelerations are in the range of between -2.17 and 1.77 m/s^2. In the warning driving situation, the deceleration range is greater than -4 m/s^2. If the monitor choose the dangerous driving condition, the desired acceleration range is greater than -8m/s^2. The desired acceleration value is calculated through Eq. (8) [11].

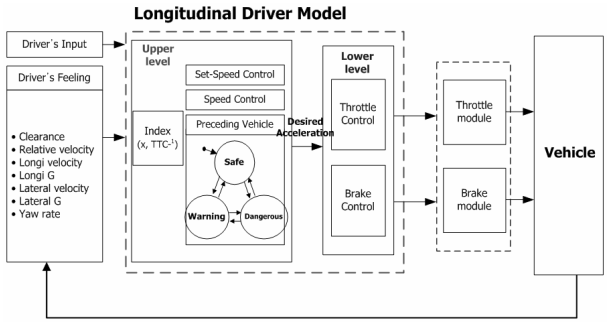

Fig. 4. Structure of the longitudinal human driver model.

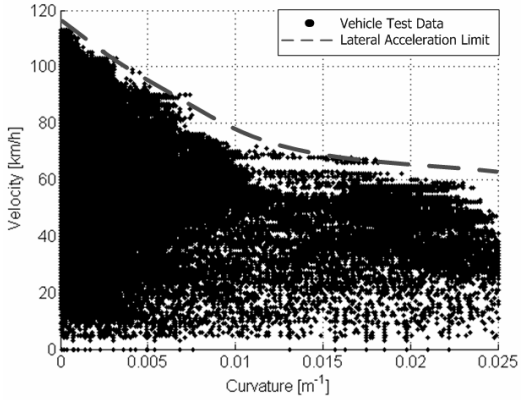

Fig. 5. Velocity tendency relative to the road curvature.

$$a_{des\_long}(t) = W_1(v_c)\cdot a_1(x) + W_2(v_c)\cdot a_2(TTC^{-1}) \tag{8}$$

where $a_1(\bullet)$ and $a_2(\bullet)$ are the functions defined by the warning index and the inverse *TTC*, respectively, and W_i is the weighting factor defined as a function of the vehicle speed.

The low-level controller manipulates the throttle/brake actuators such that the vehicle acceleration tracks the desired acceleration. The throttle/brake control is based on the reverse dynamics. [12]

2.3 Curvature-based human driver model

To consider road curvature in the throttle/brake control, the curvature-based human driver model calculates another desired acceleration (a_{des_curv}). In a curved road driving situation, a driver tends to maintain a one's safety velocity (v_{safe}) range. This tendency is confirmed in Fig. 5.

This tendency can be represented in a lateral acceleration ($a_{y,\lim}$), as shown by the dotted line in Fig. 5. Its values can be determined through Eq. (9).

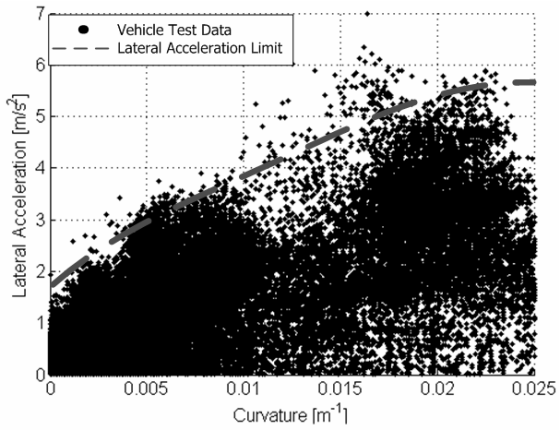

Fig. 6. Lateral acceleration tendency relative to the road curvature.

$$a_{y,lim} = \frac{v_{safe}}{R} \tag{9}$$

The curvature-based human driver model chooses a desired acceleration in the range of a lateral acceleration limit. The driver's lateral acceleration tendency in various road curvatures is depicted in Fig. 6. The dotted line in Fig. 6 is the lateral acceleration limit in the curvature-based human driver model.

The desired acceleration (a_{des_curv}) is defined as:

$$a_{des\_curv} = \frac{\Delta v}{\Delta t} = \frac{v_{des} - v_c}{T_p} \tag{10}$$

where v_{des} is the desired velocity. To represent a driver's preview distance change by velocity, the weighting factor and lateral acceleration limit values of each preview positions are used. The weighting factor is defined as a function of the vehicle speed range.

$$v_{des} = \omega_1 \cdot v_{des,1} + \cdots + \omega_N \cdot v_{des,N} \quad \left(where \quad \sum_{i=1}^{N} \omega_i = 1,\ v_{des,i} = \sqrt{a_{y\_\lim,i} \cdot R} \right) \tag{11}$$

Substituting (4) with (11), the curvature-based human driver model's desired acceleration can be obtained as through (12).

$$a_{des\_cur} = \frac{v_{des} - v_c}{\frac{L_p}{v_c}} = \frac{v_c\left(v_{des} - v_c\right)}{L_p} \quad \left(\because T_p = \frac{L_p}{v_x} = \frac{L_p}{v_c} \right) \tag{12}$$

To guarantee the safety motions of a vehicle, the final desired acceleration is defined as the minimum value between two desired acceleration, that is longitudinal human driver model's desired acceleration (a_{des_long}) and the curvature-based human driver model's desired values (a_{des_curv}).

$$a_{des} = \min\left(a_{des\_long},\ a_{des\_curv}\right) \tag{13}$$

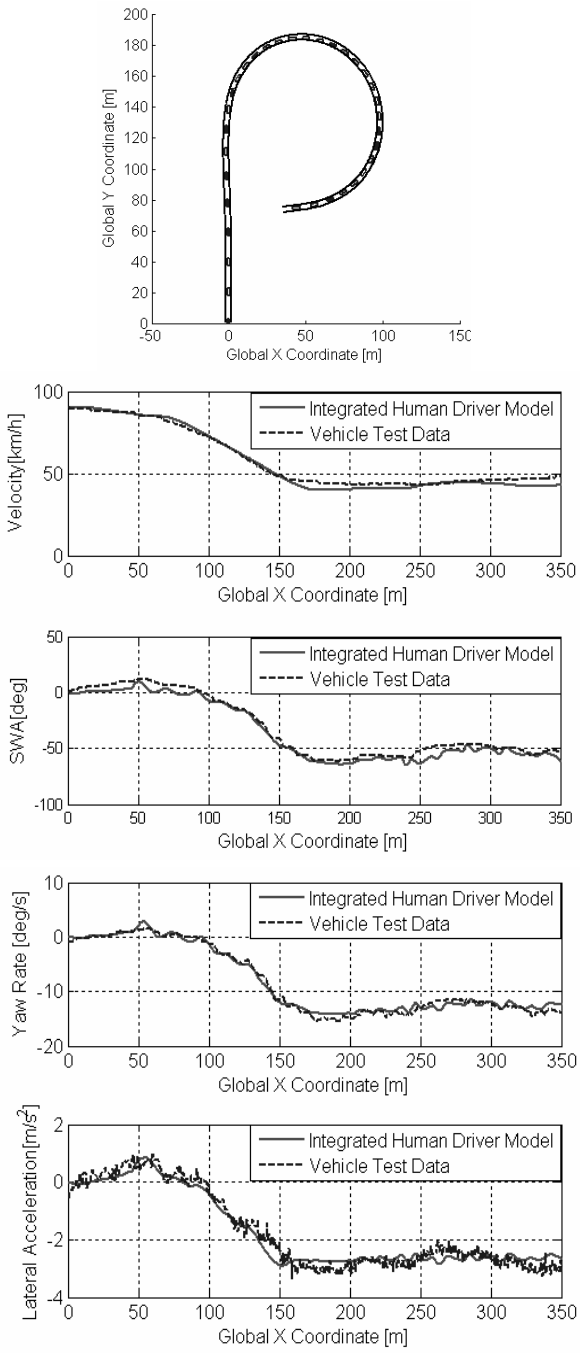

Fig. 7. Comparisons between the integrated human driver model and vehicle test data (P-shape road).

3. Validation of the integrated human driver model using manual driving data

The proposed control strategy was compared with human manual driving. The human manual driving data were collected using a test vehicle. Comparisons between integrated human driver model and a test driver's manual driving in the case where there is no preceding vehicle on a high-speed city highway were conducted on a P-shaped road. A similar case with no preceding vehicle was also tested using the integrated hu-

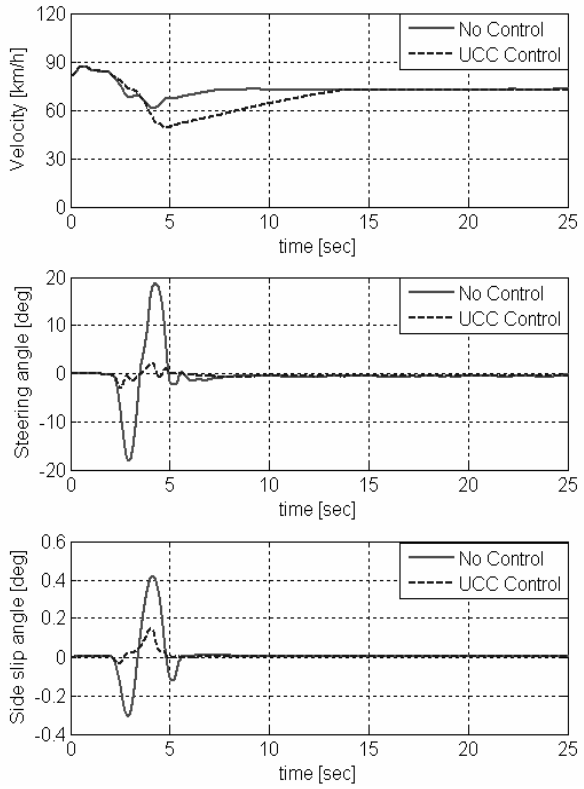

Fig. 8. Comparison of the UCC vs. No control.

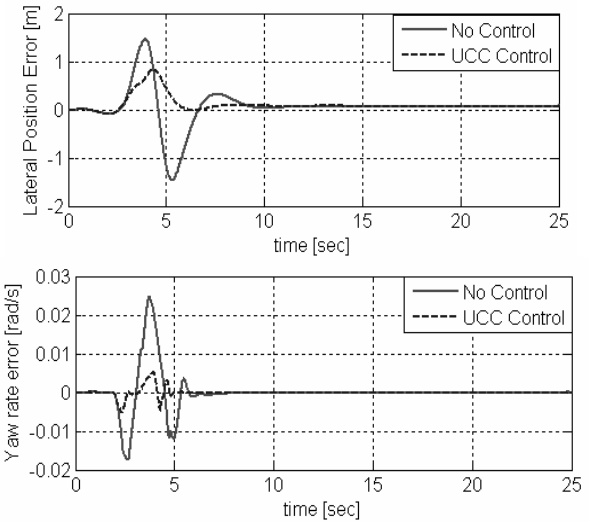

Fig. 9. Vehicle trajectory and error of UCC vs. No control.

man driver model. The simulation results and data from the real driver's test are shown in Fig. 7.

As shown in Fig. 7, vehicle velocity, steering, yaw rate and lateral acceleration are controlled in the same way as in a real driver's maneuver control case. Based on these results, the integrated human driver model could control the vehicle in the same way as a real driver could in various curvature road conditions.

4. Closed-loop simulation of unified chassis controller

In this section, a closed-loop simulation with the integrated human driver model was conducted to investigate the performance of a UCC in comparison with "no control" situation. To improve the vehicle's lateral stability and maneuverability, the UCC was developed by integrating individual chassis control modules such as Electronic Stability Control (ESC), Active front steering (AFS) and Continuous Damping Control (CDC). The UCC controller's control input is decided based on the driver's steering input, friction circle, and desired yaw moment values [13].

The test road was a 300*m* radius of the road curvature after a straight road, and the split mu was located at the entrance of a curved section. The initial vehicle speed was set a *90km/h*.

Figs. 8 and 9 show the simulation results on the vehicle. Fig. 9 shows that both the UCC and the no control scenario have a good tracking reference trajectory but the no control case demonstrates an insecure behavior on the split mu section. However, the UCC has better performance at the yaw rate and the side slip angle than in the no control case. While the driver's steering angle in UCC is smaller than that in the no control case.

The results show that the closed-loop simulation with the integrated human driver model can be used to test the UCC controller's performance. This can lead to the improvement of a vehicle's lateral stability and maneuverability.

5. Conclusions

An integrated human driver model for closed-loop simulation of an intelligent safety system has been presented. The control algorithm has been designed to achieve realistic behavior of a human driver in a normal driving situation. To represent a driver's steering motion and throttle/brake motion, the integrated human driver model is constructed in three submodes: lateral human driver model, longitudinal human driver model and curvature-based human driver model. The lateral human driver model decides a driver's steering angle by using the finite optimal preview control method. The driver's throttle/brake control motion is controlled with the desired accelerations which are calculated using the longitudinal human driver model and curvature-based human driver model.

It has been shown that the proposed integrated human driver model can control a vehicle in the same way human manual driving does in various road curvature situations. It can also represent a normal driver's driving motion. Consequently, the integrated human driver model presented in this study can be used into a closed-loop simulation and for the development of a vehicle's intelligent safety system.

Acknowledgment

This work was partially supported by the Korea Automotive Technology Institute (KATECH), the BK21 program of the

Korea Research Foundation Grant funded by the Korean Government (MEST) (KRF-2009-200-D00003), and the National Research Foundation of Korea Grant funded by the Korean Government (2009-0083495) and SNU-IAMD.

Nomenclature

y_r	:	Lateral position error
C	:	Center of gravity
ε	:	Yaw angle
ε_d	:	Desired yaw angle
w	:	Preceding vehicle's width
r_d	:	Clearance between preceding vehicle and driver's view angle
θ	:	Driver's view angle
v_x	:	Longitudinal Velocity
v_y	:	Lateral Velocity
R	:	Radius of the road
r	:	Clearance
L_p	:	Driver's preview distance
T_p	:	Preview time
m	:	Vehicle mass
I_z	:	Yaw moment of inertia
l_f	:	Distance from the center of gravity to front axle
l_r	:	Distance from the center of gravity to front axle
C_f	:	Cornering stiffness of the front tire
C_r	:	Cornering stiffness of the rear tire
a_{des_long}	:	Desired acceleration based on preceding vehicle
a_{des_curv}	:	Desired acceleration based on road curvature
$a_{y\_\lim}$	:	Lateral acceleration limitation
v_{safe}	:	Driver's safety velocity
v_{des}	:	Desired velocity based on road curvature
v_c	:	Current velocity
a_{des}	:	Final Desired acceleration

References

[1] D. J. G. James, F. Boehringer, K. J. Burnham and D. G. Copp., *Adaptive driver model using a neural network*, Artificial Life and Robotics, Springer Japan, 7 (4) (2004).

[2] M. C. Nechyba and Y. Xu, Human Control Strategy, Abstraction, Verification, and Replication, *IEEE Control Systems Magazine*, (1997) 48-61.

[3] Tatsuya Suzuki and Shinkichi Inagaki, et al,. Modeling and Analysis of Vehicle Following Task based on Mode Segmentation, *AVEC 08, 9th International Symposium on Advanced Vehicle Control*, (2008) 614-619.

[4] Hung Pham, Karl Hedrick and Masayoshi Tomizuka, Combined Lateral and Longitudinal Control of Vehicles for IVHS, *American Control Conference*, 2 (1994) 1205-1206.

[5] Rajesh Rajamani, Han-Shue Tan, Boon Kait Law and Wei-Bin Zhang, *Demonstration of Integrated Longitudinal and Lateral Control for the Operation of Automated Vehicles in Platoons, IEEE*, Vol.8, Control Systems Technology, (2000) 695-708.

[6] Kang, JuYong, Yi, Kyongsu and Noh, Kihan, Development and Validation of a Finite Preview Optimal Control-based Human Driver Steering Model, *KSME Spring Conference in 2007, KSME*, (2007) 130-135.

[7] H. Peng, *Vehicle Lateral Control for Highway Automation. Ph.D Thesis*, University of California at Berkeley, (1992).

[8] H. Peng and M. Tomizuka, Lateral Control of Front-Wheel-Steering. Rubber-Tire Vehicles, *Publication of PATH project, ITS, UC Berkeley*, UCB-ITS-PRR-90-5 (1990).

[9] Chen, Long-Chain, *An active suspension system with preview control for passenger automobiles. PhD Thesis*, Massachusetts Institute of Technology, (1988).

[10] Burl, Jeffrey B. Linear Optimal Control, pp.179-226, *Addison-Wesley Longman*, Boston, MA. (1998).

[11] Seungwuk Moon and Kyongsu Yi, Human driving data-based Design of a Vehicle Adaptive Cruise Control Algorithm, *Vehicle System Dynamics*, 46 (8) (2008) 661-690.

[12] K. Yi and I. Moon, A driver-adaptive range policy for adaptive cruise control, IMechE, Part D: *J. Automobile Engineering*, 220 (2006) 321-334.

[13] Wanki Cho, Jangyeol Yoon, Jeongtae Kim, Jaewoong Hur and Kyongsu Yi, An Investigation into Unified Chassis Control Scheme for Optimized Vehicle Stability and Maneuverability, *International Association of Vehicle System Dynamics, Vehicle System Dynamics*, (supplement), (46) (2008) 87-105.

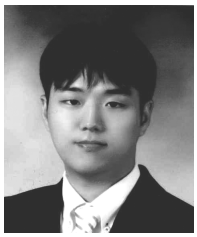

Taeyoung Lee received his B.S. degrees in mechanical and aerospace engineering from Seoul National University, Korea, in 2007. He is a Ph.D student in mechanical and aerospace engineering at the Seoul National University, Korea. His research interest is on the development of a human driver model.

Juyong Kang received his B.S. and M.S. degrees in mechanical engineering and mechanical design engineering from Hanyang University, Korea, in 2005 and 2007, respectively. He is a Ph.D. candidate in mechanical and aerospace engineering at the Seoul National University, Korea. His research interest is on autonomous robot vehicle.

Kyongsu Yi received his B.S. and M.S. degrees in mechanical engineering from Seoul National University, Korea, in 1985 and 1987, respectively, and his Ph.D. degree in mechanical engineering from the University of California, Berkeley, in 1992. Dr. Yi is a Professor at the School of Mechanical and Aerospace Engineering at Seoul National University, Korea. He currently serves as a member of the editorial boards of the KSME, IJAT and ICROS journals. Dr. Yi's research interests are control systems, driver assistant systems, and active safety systems of a ground vehicle.

Kihan Noh received his B.S. degree in mechanical engin-eering from Pusan National University, Korea, in 1995. He obtained his M.S. degree from Department of Mechatronics of GIST, Korea, in 1997. He is currently a doctorate course in KAIST. Mr. Noh is currently the Head (Team Manager) of the Vehicle Platform Research Center of Intelligent Vehicle Technology R&D Division at Korea Automotive Technology Institute (KATECH) in Chonan, Korea. His research interests include vehicle dynamics and control, human factors, and HILS-based evaluation technology.